IMPULSIVE NOISE MITIGATION IN SPATIAL AND TEMPORAL DOMAINS FOR SURFACE-WAVE OVER-THE-HORIZON RADAR

Yuri I. Abramovich, Pavel Turcaj

CSSIP
SPRI Building
Technology Park Adelaide
Mawson Lakes
SA 5095, Australia
yuri@cssip.edu.au, pavel@cssip.edu.au

ABSTRACT

Surface-wave over-the-horizon radars, especially ones located in tropical areas, such as Northern Australia, are usually strongly affected by external impulsive noise. Apart from thunderstorm activity, man-made (industrial) noise over typically quite long coherent-integration time often is of impulsive nature as well.

In this paper we analyse the efficiency of temporal and spatial adaptive techniques for impulsive noise mitigation. We demonstrate that for heavily contaminated dwells, new spatio-temporal adaptive processing is most effective. Initial impulsive noise mitigation, produced by adaptive spatial processing is used for range and azimuth dependent sea-clutter spectrum estimation. Estimated sea-clutter spectrum is then used to "restore" the "missing" data, originally contaminated by impulsive noise.

1. DESCRIPTION AND ANALYSIS OF MITIGATION TECHNIQUES

The High Frequency Over-the-Horizon Radar (HF OTHR) probably constitutes the most prominent example of radars subjected to severe impulsive noise interference. Tropical thunderstorms which are extremely active in equatorial regions such as Northern Australia, typically generate a significant number of lightning strikes within the operational range of HF OTHR due to relatively long coherent processing intervals. In [2] based on experimental data collected in Northern Australia, we introduced point process models for atmospheric noise adequate to spatial and temporal adaptive impulsive noise mitigation. It has been suggested that optimal mitigation technique should incorporate both spatial and temporal domains based on the properties of particular lightning strike.

Our recent experimental trial conducted from May to September 2000 in Northern Australia revealed that accidental human-made noise that quite often interferes with a HF radar, is in most cases also highly nonstationary. The atmospheric strike typically occupies a single repetition period or at most a few consecutive repetition periods (for high air-mode waveform repetition frequencies WRF=40 - 60 Hz), man-made impulsive interference typically occupies significantly longer intervals, measured in dozens of repetition periods (sweeps). Typical examples of atmospheric and man-made impulsive noise are presented in Fig. 1, 2. The amplitude of the range processed data at the output of one particular beam are shown for different ranges (y-axis) as a function of repetition period (x-axis). One can see significant difference in number of sweeps contaminated by atmospheric and man-made impulsive noise. Another important feature demonstrated by these figures is the availability of "sea clutter-free ranges". These ranges allow for straight-forward identification of sweeps affected by impulsive noise.

Obviously, analysis of impulsive noise mitigation efficiency should be expanded to man-made interference. Indeed, since only up to 30% of entire dwell is typically corrupted, there is a reason to compare spatial techniques with temporal ones[1].

In this paper we introduce comparative analysis of different temporal and spatial adaptive techniques, suitable for impulsive noise mitigation.

Since the actual interval corrupted by impulsive noise is easily identified, temporal techniques are focused on a proper estimation of the missing sea-clutter data. For surface-wave radars with typically very high sub-clutter visibility that can range far above 60 dB, an accurate estimation can become a problem.

To address this problem two major approaches could be adopted. The first one is based on classical Weiner prediction filter. Complicated nature and range/azimuth variability of sea-clutter Doppler spectrum impose limitations on the actual accuracy of this approach.

The second technique is based on direct optimization of replacement data to minimize the total power within the specified range of Doppler frequencies which are expected to be free of sea clutter. This technique has a different limitations, especially when the number of missing data is quite large and consecutive. However, in attempt to minimize the overall power, strong targets could be suppressed and some important features of the sea-clutter spectrum could be significantly damaged. Spatial techniques are effective when strong impulsive interference impinges on a beampattern sidelobes. Meantime, when the entire coverage is important, there would always exist directions corrupted by impulsive noise propagated via the main beam.

Comparative analysis of the above mentioned techniques was done firstly on uncorrupted SW OTHR data with subclutter visibility close to the limit. One selected example is shown in Fig. 3. A certain number of sweeps has been nominated as being "corrupted" and two abovementioned temporal techniques have been used to restore the "missing" data.

In order to apply the classic prediction (interpolation) approach, we first estimated the sea-clutter temporal covariance matrix. With

$N = 1000$ repetition periods typically used in ship mode, we selected $M < N/2$, $M = 400$ as a dimension of prediction/interpolation filter in expectation that whatever the actual number of missing repetition periods is, there still should be a sufficient number of uncorrupted repetition periods (sweeps) within corresponding M-variate "sliding window" of our prediction filter. The M-variate (range-dependent) sea-clutter covariance matrix is estimated here by forward-backward averaging:

$$\widehat{R}_d = \sum_{j=1}^{N-M+1} \left(X_j^d (X_j^d)^H + J\bar{X}^d{}_j X_j^{dT} J \right) \quad (1)$$

where

$$X_j^d = (x_j^d, x_{j+1}^d, \ldots, x_{j+M}^d) \quad (2)$$

$$J = \begin{bmatrix} 0, & \ldots & ,1 \\ \vdots & \ddots & \vdots \\ 1, & \ldots & ,0 \end{bmatrix}, \quad (3)$$

and x_j^d is the complex number that corresponds to j-th repetition period and d-th range cell. Particular beam number is not essential for this temporal processing.

Let us introduce an $M \times (M - m)$ variate incidence matrix H_m that is constructed as standard identity matrix with m deleted rows at positions that correspond to the "missing" sweeps. Then the adaptive prediction filter that generates an estimate of the k-th missing data is defined as

$$W_k^d = \left[H_m^T \widehat{R}_d H_m \right]^{-1} H_m r_k^d, \quad k = 1, \ldots, m \quad (4)$$

where r_k^d is k-th column of the M-variate matrix $\widehat{R}_d$.

Correspondingly, the estimate $\widehat{x}_k^d, \quad k = 1, \ldots, m$ of th k-th missing sweep is defined as

$$\widehat{x}_k^d = W_k^{dH} H_m^T X^d, \quad k = 1, \ldots, m \quad (5)$$

Our second approach is based on direct search for the m-variate vector $\widehat{X}_m$ for "missing" data that with respect to the remaining $(N - m)$ "valid" data results in the minimal total power within some designated range of Doppler frequencies.

Specifically let us present the overall N-variate vector X^d as

$$X^d = X_0^d + \mathsf{A}_m \widehat{x}_m \quad (6)$$

here X_0^d is a N-variate vector with zeroes the positions of "missing" data, A_m is $N \times m$-variate incidence matrix, where rows of the m-variate matrix are "spread" over N rows, corresponding to the positions of the missing data.

Weighted Discrete Fourier Transform (DFT) over the vector X^d could be presented as

$$FD(X_0^d + \mathsf{A}_m \widehat{x}_m) \quad (7)$$

and with $(N - n) \times N$ selection matrix S, the $(N - m)$-variate vector of selected Doppler bins within the d-th range Doppler spectrum could be presented as

$$SFD(X_0^d + \mathsf{A}_m \widehat{x}_m) \quad (8)$$

where F is the N-variate DFT matrix, D is a diagonal weighting matrix (e.g. Blackman window).

Finally, the overall power within this Doppler window could be presented as

$$X_0^{dH} DF^H SS^T FDX_0^d + \widehat{x}_m^H \mathsf{A}_m^H DF^H SS^T D\mathsf{A}_m \widehat{x}_m + \quad (9)$$

$$cr\widehat{x}_m^H \mathsf{A}_m^H DF^H SS^T FDX_0^d + X_0^{dH} DF^H SS^T FD\mathsf{A}_m \widehat{x}_m. \quad (10)$$

Correspondingly the optimum solution is

$$\widehat{x}_m = -[\mathsf{A}_m^H DF^H SS^T FD\mathsf{A}_m]^{-1} \mathsf{A}_m^H DF^H SS^T DX_0^d. \quad (11)$$

(For rank deficient matrix $[\mathsf{A}_m^H DF^H SS^T FD\mathsf{A}_m]$ this solution is modified to operate on signal subspace of this matrix.) Now these techniques could be compared. Fig 4 presents the Doppler spectra for $m = 100$ of "missing" data for one range cut. Both random (atmospheric like) and continuous (man-made like) distributions of "missing" data within the 400 sweeps long window have been analysed. Different number of missing sweeps have been analysed, $m = 1, 40, 60, 100$, however only $m = 100$ continuous case processed with optimization filter is shown (the only one which shows any difference from the original).

The results demonstrate that for randomly distributed "missing" data both techniques provide equally good restoration. The prediction errors are equally small and sub-clutter visibility is restored to the original level in this case. However in the case of continuous "missing" data both methods work equally well only for a small number of "missing" sweeps. For increased number of consecutive missing data the difference between these two techniques becomes more significant. While classical prediction is still efficiently restoring missing data (up to 100 of missing data for 400-variate prediction filter), optimization (11) generates estimates $\widehat{x}_m$ significantly different from the true missing ones. These estimates lead to reduction in overall noise power within the specified Doppler area, but the overall structure of the Doppler spectrum changes significantly. For most practical applications these changes could not be tolerated. Moreover, with significant number of "degrees of freedom", total power minimization could considerably reduce the target signal as well. Thus, for a randomly distributed missing data or small number of consecutive missing data (up to 20 consecutive sweeps) the optimization technique (11) could be recommended as a preferred option since it does not involve (adaptive) sea-clutter spectrum estimation. For typical man-made impulsive interferences, this approach is not appropriate and attention should be attracted to a practical implementation of adaptive prediction technique (4)-(5). Main problem here is to get an accurate enough estimate for the sea clutter covariance matrix $\widehat{R}_d$. Since the dimension of this matrix (prediction filter) should be significantly greater than the number of missing sweeps - real (corrupted) data should not be used directly for sample matrix estimation (1) in the way it has been done in our previous study with uncorrupted data. Since all ranges are usually equally corrupted by impulsive noise, spatial diversity could be explored to assist sea-clutter covariance matrix estimation. Indeed, in most cases truly dominant impulsive noise sources are well localized and even with conventional beamformer it is usually possible to find the least contaminated direction (beam). While Fig 2 displays the range map for the most occupied beam, the top line in Fig 6 demonstrates distribution of this impulsive noise power-to-noise ratio across the beams. It is quite obvious, that in the "minimal" beam (N=7) the power of this noise is significantly smaller and range processed data of this beam could be used for covariance matrix estimation. Obviously, adaptive spatial processing is even more effective in terms of reduction of antenna pattern sidelobes

affected by impulsive noise. The bottom line in Fig 6 presents the similar impulsive noise to white noise ratio as a function of beam direction for spatial adaptive processing (SAP). Here sea clutter-free ranges are used to estimate sample spatial covariance matrix $\widehat{R}_{sp}$;

$$\widehat{R}_{sp} = \sum_{d,j\in\theta} X_{d,j}^{sp} X_{d,j}^{spH} \tag{12}$$

where

$$X_{d,j}^{sp} = (x_{d,j}^{(1)}, \ldots, x_{d,j}^{(32)})^T \tag{13}$$

θ is the sea-clutter free ranges area and SAP beamformer is defined as usual by

$$\widehat{W}_{SAP}(l) = \frac{\widehat{R}_{SP}^{-1} S_l}{S_l^H \widehat{R}_{SP}^{-1} S_l} \tag{14}$$

with S_l as a 32-variate steering vector.

The most important issue that needs to be addressed to justify this approach is sensitivity of this technique with respect to sea-clutter azimuthal variability. Indeed, we are prepared to use the sea clutter training data collected at the output of one particular (adaptive) beam, but apply it to quite a different (conventional) beamformer output. In order to investigate the efficiency of such technique, we analysed our "clean" data with nominated "missing" data. For Weiner prediction filter there is no visible difference for one range-doppler cut between the original data and restored ones even for quite large number of missing data (m=100), regardless of the fact if the data are random or consecutive. For the optimization filter the same can be said for random distribution of the replaced sweeps However the same cannot be said for consecutive sweeps as the inverted matrix becomes ill conditioned. The Fig 4 demonstrates, there is some degradation of the signal in the "sea clutter" area

Finally we illustrate the practical efficiency of our approach buy processing the real contaminated data shown in Fig 1,2.

For the data shown in Fig 1 optimization technique (11) should be appropriate since only one dominant "strike" is recorded here.

The results of this technique applied to one beam Fig 5 demonstrate quite impressive improvement in sub-clutter visibility. Particular range profile shown in Fig 7 demonstrates 35 dB improvement in sub-clutter visibility, while the standard SAP has delivered only mere 8-10 dB

Our second example deals with the man-made impulsive noise, as per Fig 2 While SAP is practically not effective for the data collected at the direction of impulsive noise arrival (beam 4) it provides quite reasonable improvement for beam 7 data that thus could be used as training one The above described approach with adaptive prediction filter "trained" on beam 7 data and applied to beam four data is illustrated by Fig 8. The particular range profile demonstrates improvement in sub-clutter visibility up to 20 dB. Note that quite significant part of coherent processing interval (CPI) has been contaminated here. Interestingly enough, when the same prediction filter is applied to the training data of the beam 7 (Fig 9), still considerable additional improvement with respect to the SAP processing has been obtained. The reason behind becomes clear when sea clutter free ranges processed by SAP are analysed: impulsive noise residues are still some 10 dB above the ambient noise floor. Therefore the replacement of these corrupted repetition intervals by predicted ones results in additional improvement in sub-clutter visibility.

2. CONCLUSION

Analysis of selected temporal and spatial adaptive techniques for atmospheric and man-made impulsive noise mitigation for SW OTHR has been performed. It has been demonstrated that temporal or spatial only processing could be effective only in special cases. For contaminated repetition periods which are randomly distributed over CPI, direct optimization method is shown to be very effective. For some beam directions affected by impulsive noise via antenna pattern sidelobes, standard spatial adaptive processing could be also quite effective on its own. In more general case, when the number of contaminated sweeps is quite significant and consecutive (man-made impulsive noise), and impulsive noise must be rejected in all directions, proposed spatio-temporal adaptive processing is shown to be most effective. Here spatial (adaptive) processing is used for initial impulsive noise mitigation, and the beam where this reduction is maximal is used as a training one for sea-clutter (temporal) covariance matrix estimation. Adaptive Weiner filter trained by the spatially processed data is then applied to contaminated (conventionally) beamformed data with similar energetic content of Doppler spectra.

3. REFERENCES

[1] Y.I. Abramovich, J.F. Böhme, A.Y. Gorokhov, and D. Maiwald. GEM-algorithm for sea echo Doppler analysis with data corrupted by sparkling interference. In *Proc. of the SPIE*, pages 194–203, San Diego, 1993.

[2] Y.I. Abramovich, N.K. Spencer, and S.J. Anderson. Experimental trials on non-Gaussian environmental noise mitigation for surface-wave over-the-horizon radar by adaptive antenna array processing. In *Proc. HOS-99*, pages 340–344, Ceasarea, 1999.

Figure 1: Atmospheric impulsive noise, beam 1.

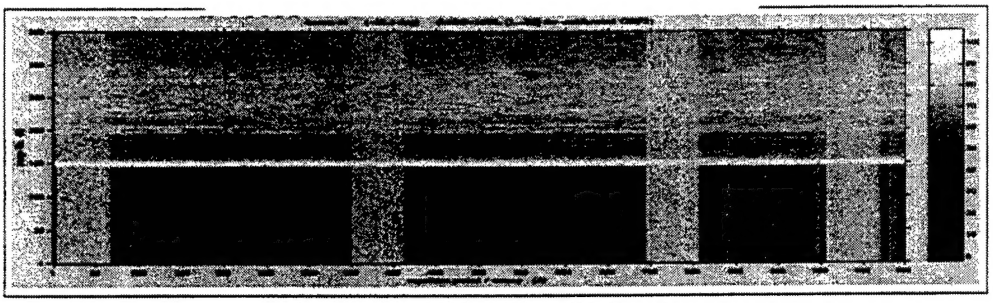

Figure 2: Man-made impulsive noise, beam 4.

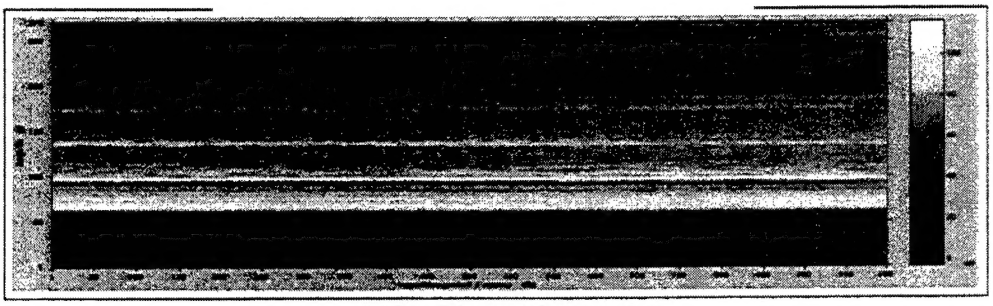

Figure 3: "Clean" data used for comparison.

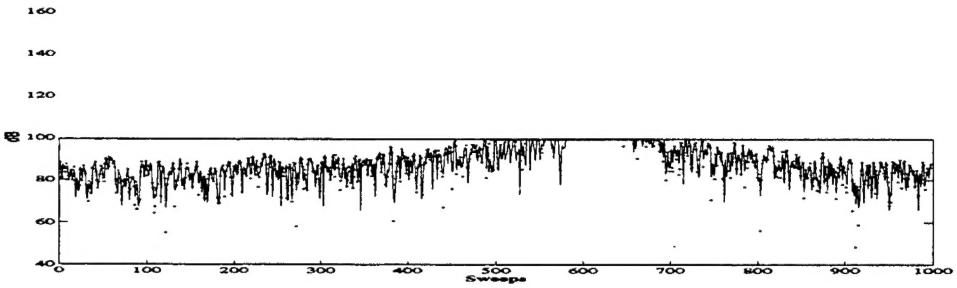

Figure 4: Comparison of original data and optimization filter with 100 consecutive sweeps replaced.

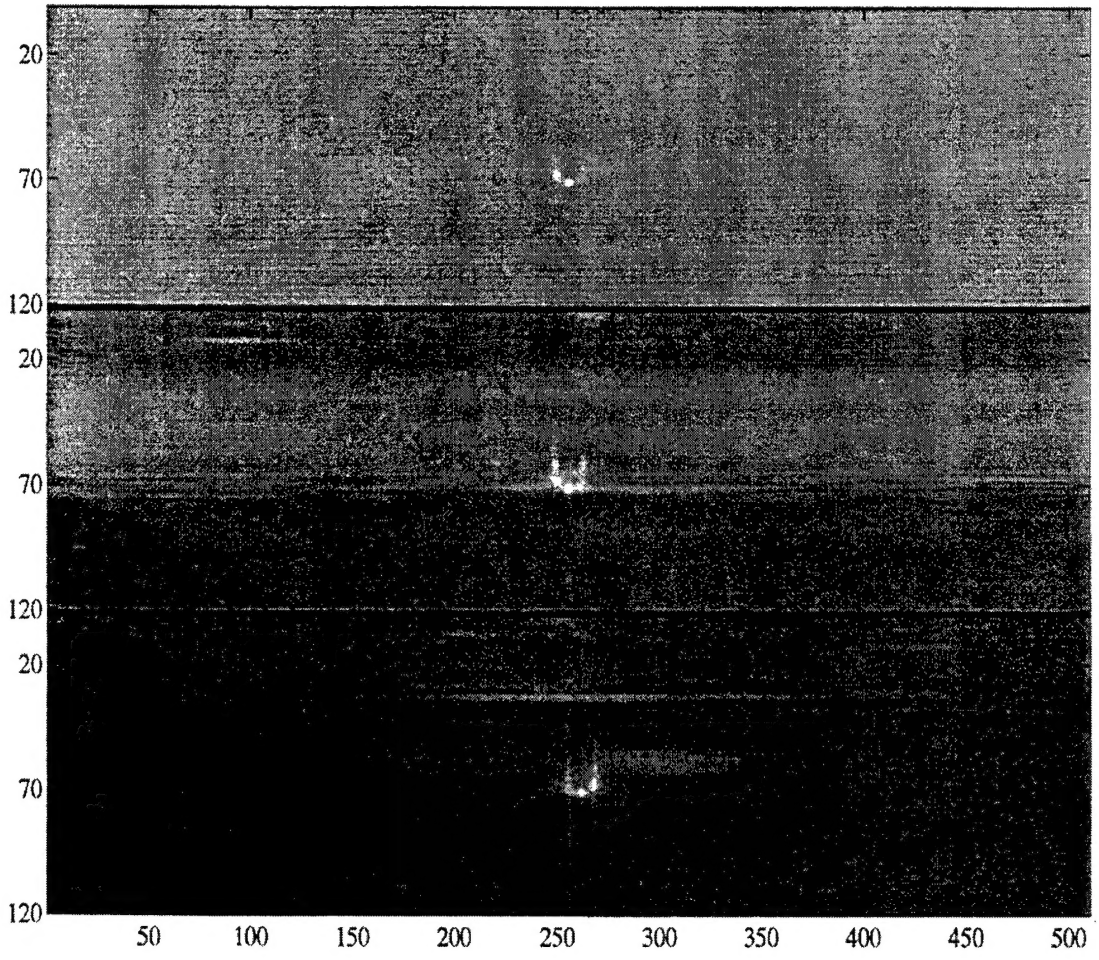

Figure 5: Comparison of conventional, SAP and optimization beamformer.

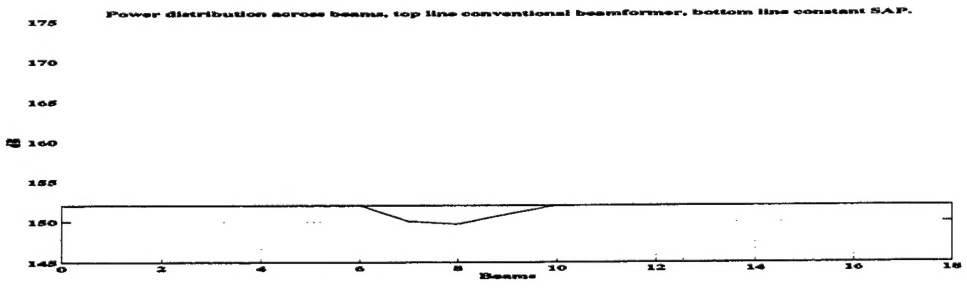

Figure 6: Power distribution accross beams, top convetional beamformer, bottom SAP.

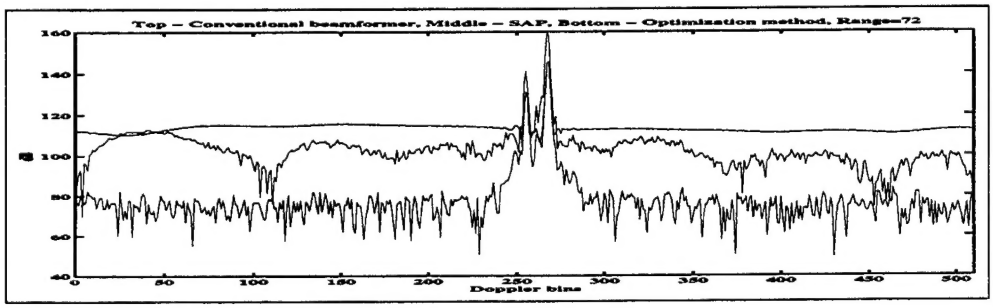

Figure 7: One range cross section, top-original,middle-SAP,bottom-optimization

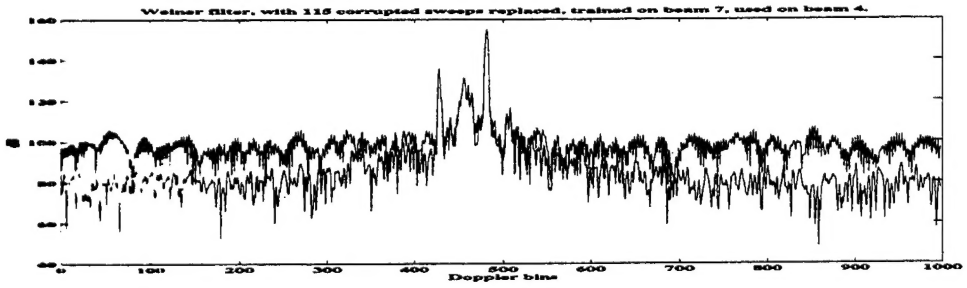

Figure 8: Weiner prediction filter trained on beam 7, used on beam 4.

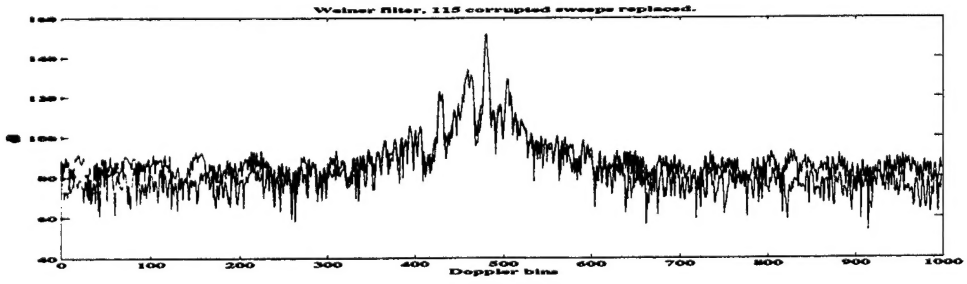

Figure 9: Weiner prediction filter trainde on beam 7, used on beam 7 top line - SAP bottom line - Weiner prediction filter.